ACS APPLIED MATERIALS & INTERFACES

Research Article

www.acsami.org

First-Principles Study on the Thermal Stability of $LiNiO_2$ Materials Coated by Amorphous Al_2O_3 with Atomic Layer Thickness

Joonhee Kang[†] and Byungchan Han*[,‡]

[†]Department of Energy Systems Engineering, DGIST, Daegu 711-873, Republic of Korea

[‡]Department of Chemical and Biomolecular Engineering, Yonsei University, Seoul 120-749, Republic of Korea

Supporting Information

ABSTRACT: Using first-principles calculations, we study how to enhance thermal stability of high Ni compositional cathodes in Li-ion battery application. Using the archetype material $LiNiO_2$ (LNO), we identify that ultrathin coating of Al_2O_3 (0001) on LNO(012) surface, which is the Li de-/intercalation channel, substantially improves the instability problem. Density functional theory calculations indicate that the Al_2O_3 deposits show phase transition from the corundum-type crystalline (c-Al_2O_3) to amorphous (a-Al_2O_3) structures as the number of coating layers reaches three. Ab initio molecular dynamic simulations on the LNO(012) surface coated by a-Al_2O_3 (about 0.88 nm) with three atomic layers oxygen gas evolution is strongly suppressed at T = 400 K. We find that the underlying mechanism is the strong contacting force at the interface between LNO(012) and Al_2O_3 deposits, which, in turn, originated from highly ionic chemical bonding of Al and O at the interface. Furthermore, we identify that thermodynamic stability of the a-Al_2O_3 is even more enhanced with Li in the layer, implying that the protection for the LNO(012) surface by the coating layer is meaningful over the charging process. Our approach contributes to the design of innovative cathode materials with not only high-energy capacity but also long-term thermal and electrochemical stability applicable for a variety of electrochemical energy devices including Li-ion batteries.

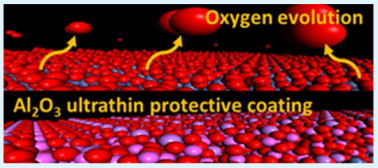

KEYWORDS: *Li-ion battery, first-principles calculations, surface coating, amorphous Al_2O_3, thermal stability*

INTRODUCTION

A Li-ion battery (LIB) has been extensively utilized to empower locomotive electric vehicles and portable electronic devices. Recently, it was also considered promising for storing large-scale electric energies connected with renewable energy systems through a smart grid network.[1,2] While the high energy capacity and power density of LIB have been substantially improved over the last several decades, still long-term electrochemical and thermal stability remain unsolved issues.[3,4] This was largely ascribed to unfavorable interface reactions between the electrolyte and electrode of the LIB system. For example, it was reported that conventional liquid-phase organic electrolytes had potential risks to inflame at high operational voltage conditions,[5,6] whereas cathodes with high Ni compositions were seriously damaged by thermal instability.[7,8]

Recently, it was reported that surface coatings on the electrodes with thin oxides could improve the durability.[9−16] For example, Lee and co-workers[12,13] demonstrated that ultrathin Al_2O_3 layers on $LiCoO_2$ coated by atomic layer deposition (ALD) enhanced both the cycling performance and the lifetime of LIB in a liquid electrolyte environment. Similar benefits were also reported for $Li[Ni,Co,Mn]O_2$[14] and in Li-excessed $Li[Li,Ni,Co,Mn]O_2$[15,16] cathodes. It was speculated that Al_2O_3 layers suppressed electrochemical dissolution of transition metals via prevention of direct physical contact between the cathode and the electrolytes. However, thermal stability of cathodes in LIB application with the surface coatings has been rarely reported in previous theoretical and experimental studies.

In this paper, we studied $LiNiO_2$ (LNO) cathode with and without Al_2O_3 overlays on a (012) surface, the Li channel for the de-/intercalation process. We chose the LNO material since it is a archetype cathode showing high-energy capacity but low thermal stability resulting from substantial surface reconstruction over long period of time of LIB operation.[17,18] Using first-principles density functional theory (DFT) calculations and ab initio molecular dynamics (AIMD), we identified energetically stable interface structures between the LNO(012) surface and deposited Al_2O_3 layers as a function of the coating thickness.

COMPUTATIONAL DETAILS

Our model system was the interface between LNO(012) surface and Al_2O_3 deposits in the (0001) direction of corundum structure (α-Al_2O_3) as shown in Figure 1: $(0001)_{Al_2O_3}/(012)_{LNO}$. Experimental observation revealed that LNO cathode underwent severe structural degradation especially in the direction of Li-ion intercalation (or deintercalation) channels.[18] The unit cell of the model system was composed of 36, 36, and 72 atoms of Li, Ni, and O, respectively, for LNO(012) slab, which contacted with Al_2O_3 having 12 and 18 of Al and O atoms per each layer. First-principles DFT calculations were performed with the spin-polarized Perdew−Burke−Ernzerhof[19] exchange-correlation functionals and the projector-augmented wave[20] method, as implemented in the Vienna Ab-initio Simulation Package (VASP).[21] The Hubbard U values (GGA+U)[22] 6.70 and 6.53 eV were used for $LiNiO_2$ and $Li_{0.75}NiO_2$ in all calculations to correct the

Received: March 23, 2015
Accepted: May 18, 2015
Published: May 18, 2015

DOI: 10.1021/acsami.5b02572
ACS Appl. Mater. Interfaces 2015, 7, 11599−11603

delocalization of 3d electron states of Ni as proposed in the literature.[23] We use the gamma-centered 1 × 1 × 1 *k*-point scheme to integrate the Brillouin zone.

AIMD simulations were utilized to estimate thermal stability of the model system. The time step of a AIMD simulation was chosen to be 1 fs with 1000 time steps, except for bare LNO (2000 time steps), in the NVT ensemble under constant volume and Nose-Hoover thermostat[24] conditions.

RESULTS AND DISCUSSION

Our DFT calculations indicated that Al and O in Al_2O_3 were positioned with the ordering of the parent α-Al_2O_3 crystallinity

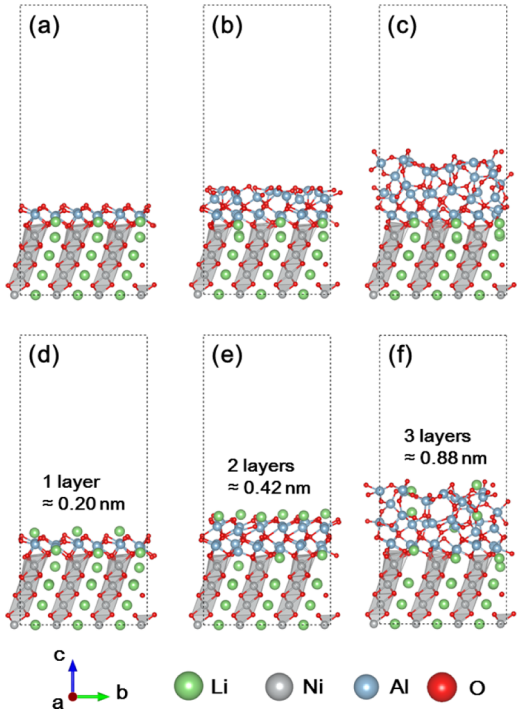

Figure 1. Interface structures of the LNO(012) surface and Al_2O_3 coatings as a function of the layer thickness. No Li inside the Al_2O_3 are depicted in (a), (b), and (c), while in (d), (e), and (f) Li was located at the outmost coating of the Al_2O_3 layer. Green, silver, light-blue, and red solid spheres mean Li, Ni, Al, and O atoms, respectively.

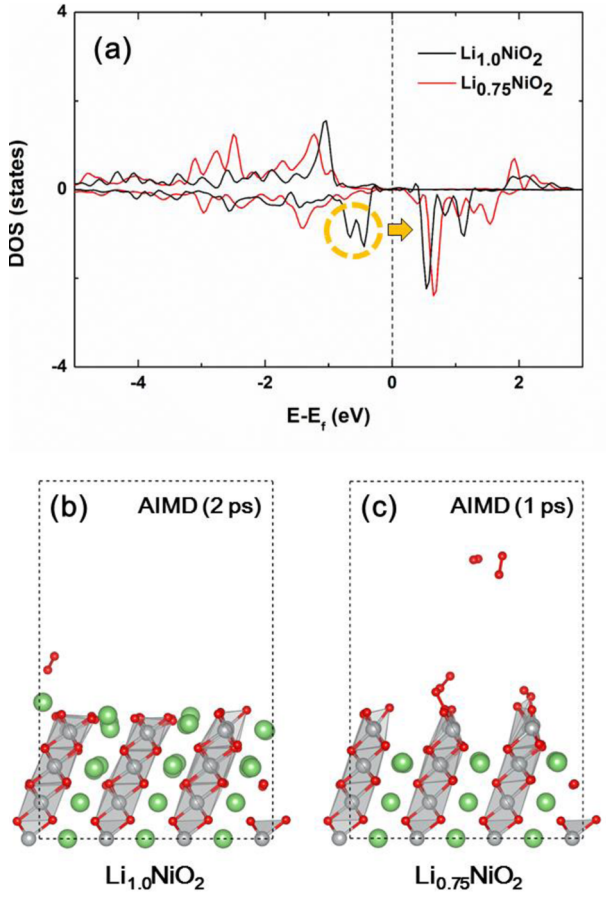

Figure 3. (a) Projected density of state for O on bare LNO(012) surface with different Li compositions. AIMD simulations at T = 400 K of $Li_{1.0}NiO_2$ in (b) and in (c) $Li_{0.75}NiO_2$ predicted both the LNO(012) surfaces are vulnerable to oxygen gas evolution but more serious in the case of less Li composition. Yellow dashed circle means that O was partially oxidized into $O^{-2+\delta}$ in a delithiated state.

if the coating thickness is less than two atomic layers (Figure 1a,b). Surprisingly, with three atomic layers Al_2O_3 was stabilized by phase transformation form the crystal to the amorphous structure (a-Al_2O_3) as shown in Figure 1c. The interlayer distance of the crystalline Al_2O_3 was about 2 Å, but 3

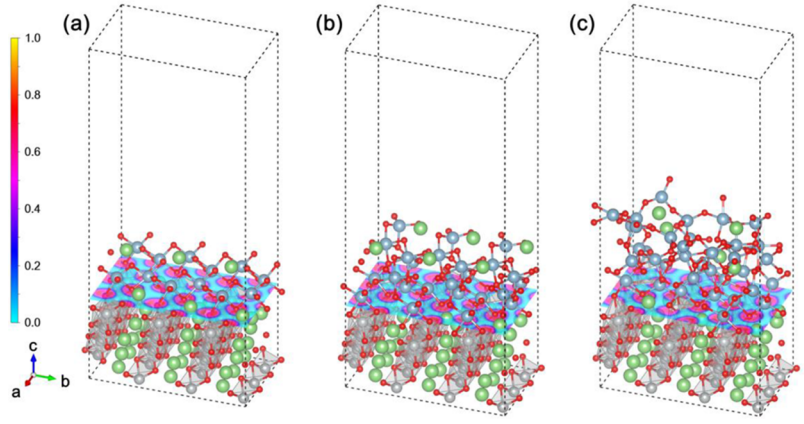

Figure 2. Profile of electron localization function (ELF) in the $(0001)_{Al_2O_3}/(012)_{LNO}$ model system with different Al_2O_3 coating thicknesses: (a) 0.20 nm, (b) 0.42 nm, and (c) 0.88 nm. The 1.0 of the numerical scale on the side bar implies complete ionic bonding between Al in the bottommost Al_2O_3 layers and O on top of the LNO(012) surface, and the lower the value, the weaker the ionic bonding character.

DOI: 10.1021/acsami.5b02572
ACS Appl. Mater. Interfaces 2015, 7, 11599−11603

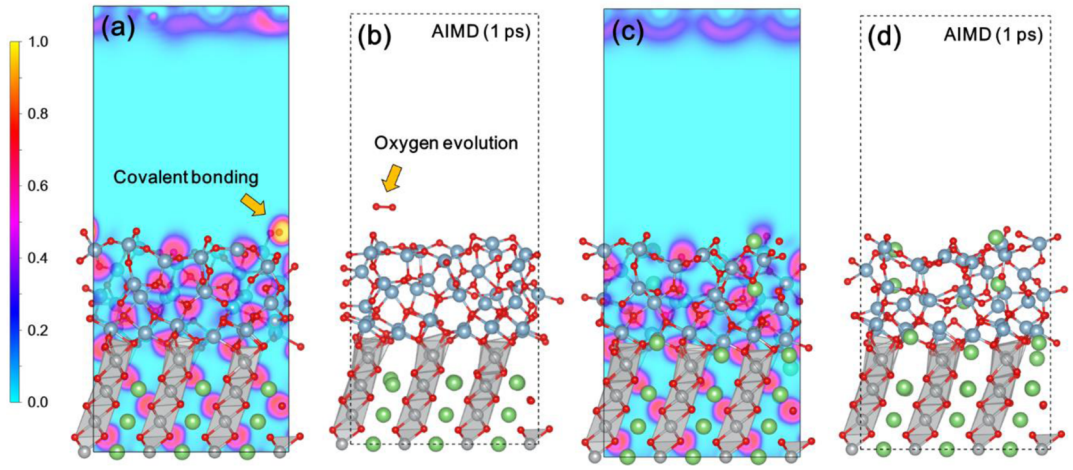

Figure 4. ELF (a, c) and AIMD simulations (b, d) in the $(0001)_{Al_2O_3}/(012)_{LNO}$ systems with and without Li atom in the Al_2O_3 coating layers. With Li in Al_2O_3 deposits (c, d) protect the LNO(012) surface versus O_2(g) evolution much better than without Li (a, b) in the layer. The underlying mechanism was analyzed by bonding characteristics between the component elements.

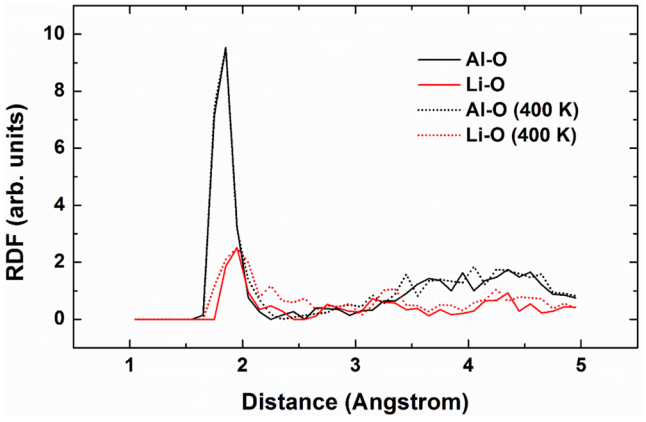

Figure 5. RDF of amorphous-phase Al_2O_3 coated on the LNO(012) surface calculated by DFT calculations (solid line) and AIMD simulations at T = 400 K (dotted line).

Å in a-Al_2O_3 due to larger free volume of the amorphous phase, which agreed well with ALD experiments at low temperatures (393−453 K).[25−30] In such temperatures, α-Al_2O_3 (corundum structure) was known as thermodynamically unstable compared to a-Al_2O_3.[31] Our DFT calculations showed that Al in the bottommost layer of a-Al_2O_3 strongly bonded to O of the LNO(012) surface as they were in the corundum structure. The Al atoms in the third layer were completely disordered.

Using the electron distribution profile calculated by the electron localization function (ELF)[32] implemented in VASP, we characterized the chemical bonding nature between Al and O near the contact interface of the model system. The ELF values range from 0 to 1, where ELF = 1 represents an entire localization of the electrons, while ELF < 0.5 means no chemical bonding. Figure 2 illustrates the ELF of Al and O as a function of Al_2O_3 coating thickness. It clearly shows that Al−O features strong ionic bonding.

To understand how the ionic bonds influenced the contact strength of $(0001)_{Al_2O_3}/(012)_{LNO}$, we calculated interface decohesion as a function of Al_2O_3 thickness. We defined interface decohesion energy, W_{de}, as eq 1

$$W_{de} = \frac{E_{LNO} + E_{Al_2O_3} - E_{inter}}{A} \quad (1)$$

where E_{LNO} and $E_{Al_2O_3}$ are total energies of the LNO(012) surface and Al_2O_3 layers, respectively. A is the interface area and E_{inter} is the total energy of the $(0001)_{Al_2O_3}/(012)_{LNO}$ interface. Our DFT calculations provided us W_{de} values of 1.91, 1.35, and 1.24 J m^{-2} for one, two, and three atomic layers of coatings, respectively. The positive decohesion energies implies that thermodynamically these two materials are stable in the formation of the interface, although the interface contact strength decreases with the thickness of the coating layer, agreeing with a previous report.[33] By increasing the number of coating layers, O in the LNO(012) surface exchanges electrons with more Al, reducing the decohesion energy. Because of the positive decohesion energies, the chemical-bonding characteristics of Al−O are still sustained in spite of the increased layer thickness.

We investigated the effect of state of charge of Li on thermodynamic stability of the interface model $(0001)_{Al_2O_3}/(012)_{LNO}$, which was rarely reported previously. Our DFT calculations indicated that Li on the LNO(012) surface thermodynamically prefer to move into the Al_2O_3 layers with different propensity depending on the thickness: −4.88, −3.00, and −4.37 eV for one, two, and three atomic layer coatings, respectively (Figure 1d,e,f). It agrees well with experimental observation[34−36] that Al_2O_3 with one or two layers were further stabilized as $Li_{3.4}Al_2O_3$, with extra Li. In addition, the ternary phase diagram for Li, Al, and O shows that high Li composition in Al_2O_3 can induce phase transformation from crystalline to amorphous structures.[37] Consequently, Li on the LNO(012) surface is thermodynamically driven to migrate into the Al_2O_3 layers, especially over the first charging process.

Using ab initio molecular dynamics (AIMD) at T = 400 K, we investigated the thermal stability of the LNO(012) surface without and with Al_2O_3 coating. First, we studied the bare LNO(012) surface at two extreme conditions of Li compositions: fully lithiated ($Li_{1.0}$) and delithiated states ($Li_{0.75}$). Figure 3a illustrates the projected density of state (DOS) of the 2p orbital of O, on the outmost LNO(012) surface, which clearly shows that O was partially oxidized into

DOI: 10.1021/acsami.5b02572
ACS Appl. Mater. Interfaces 2015, 7, 11599−11603

$O^{-2+\delta}$ in a delithiated state, leading to chemical instability. This electronic structure explains the reason why LNO materials are unstable, particularly in a delithiated state versus serious surface reconstruction from layered to rock-salt structures. Indeed, our AIMD simulations at T = 400 K showed that O_2(g) evolved from LNO(012) surface only after 1 ps in a delithiated state (Figure 3c). Therefore, both DOS and AIMD simulations consistently propose that the bare LNO(012) surface is vulnerable to thermal structural degradation when Li composition is lower than 1.0. The results of AIMD steps are depicted in Figure S1 in the Supporting Information.

In contrast, the LNO(012) surface coated by a-Al_2O_3 with Li inside showed dramatically high thermal stability as shown in Figure 4. To understand the origin, we utilized DFT calculations to obtain bond characteristics of the a-Al_2O_3 with (Figure 4a) and without (Figure 4c) Li on the outmost layer. The yellow (O−O) and red (Al−O and Li−O) colors indicate covalent and ionic bonds, respectively. Moreover, our AIMD simulations showed that O_2(g) evolved from the LNO(012) surface coated by Al_2O_3 without Li (Figure 4b), where covalent bonding is dominant. The a-Al_2O_3 with Li, however, no O_2(g) evolution was observed (Figure 4d). Consequently, our results indicate that the a-Al_2O_3 coating enhances structure stability of the LNO(012) surface by forming strong ionic bonds between Al and O located at the contacting plane. In turn, thermodynamic stability of the Al_2O_3 coating layers is substantially improved by Li within the layers, which eventually leads to better protection of the LNO(012) surface versus O_2(g). In accordance with the facts the radial distribution functions (RDF) obtained by AIMD simulations at T = 400 K indicated that bond distances of Al−O (1.85 Å) and Li−O (2.00 Å) barely changed as depicted in Figure 5. Again, it shows that the LNO(012) surface with the amorphous-phase-coated Al_2O_3 with Li inside is thermally stable.

CONCLUSION

Using first-principles DFT calculations and AIMD simulations, we characterized thermal stability of the LNO(012) surface with ultrathin Al_2O_3 coating. We identified that Al_2O_3 with one and two atomic layers in the (0001) direction of corundum was stabilized with the parent crystallinity, but phase-transformed into amorphous structure at three atomic layers. Interface decohesion energy between the LNO(012) surface and Al_2O_3 decreased with the increase of Al_2O_3 thickness but still maintained strong Al−O ionic bonding, which controlled the interface contact strength of the two materials. Our AIMD simulations and RDF consistently confirmed a-Al_2O_3 and Li composition in the coating layers are key parameters keeping the LNO(012) surface from serious degradation via O_2(g) evolution. Our work will contribute to guiding rational design of a high-performance LIB system with thermally stable materials over a long period of operation.

ASSOCIATED CONTENT

Supporting Information

Outcomes of ab initio molecular dynamic simulations for bare $LiNiO_2$ and $Li_{0.75}NiO_2$ materials at T = 400 K. The Supporting Information is available free of charge on the ACS Publications website at DOI: 10.1021/acsami.5b02572.

AUTHOR INFORMATION

Corresponding Author

*E-mail: bchan@yonsei.ac.kr.

Notes

The authors declare no competing financial interest.

ACKNOWLEDGMENTS

This research was supported by Global Frontier Program through the Global Frontier Hybrid Interface Materials (GFHIM) of the National Research Foundation of Korea (NRF) funded by the Ministry of Science, ICT & Future Planning (2013M3A6B1078882). This work was also supported by the IT R&D program of MKE/KEIT (10041856). Authors appreciate DGIST for supporting supercomputing resources for the research.

REFERENCES

(1) Armand, M.; Tarascon, J.-M. Building Better Batteries. *Nature* **2008**, *451*, 652−657.
(2) Lindley, D. Smart Grids: The Energy Storage Problem. *Nature News* **2010**, *463*, 18−20.
(3) Scrosati, B.; Garche, J. Lithium Batteries: Status, Prospects and Future. *J. Power Sources* **2010**, *195*, 2419−2430.
(4) Scrosati, B.; Hassoun, J.; Sun, Y.-K. Lithium-Ion Batteries. A Look into the Future. *Energy Environ. Sci.* **2011**, *4*, 3287−3295.
(5) Tarascon, J.-M.; Armand, M. Issues and Challenges Facing Rechargeable Lithium Batteries. *Nature* **2001**, *414*, 359−367.
(6) Wang, Q.; Ping, P.; Zhao, X.; Chu, G.; Sun, J.; Chen, C. Thermal Runaway Caused Fire and Explosion of Lithium Ion Battery. *J. Power Sources* **2012**, *208*, 210−224.
(7) Arai, H.; Okada, S.; Sakurai, Y.; Yamaki, J.-i. Thermal Behavior of $Li_{1-y}NiO_2$ and the Decomposition Mechanism. *Solid State Ionics* **1998**, *109*, 295−302.
(8) Wang, L.; Maxisch, T.; Ceder, G. A First-Principles Approach to Studying the Thermal Stability of Oxide Cathode Materials. *Chem. Mater.* **2007**, *19*, 543−552.
(9) Jung, Y. S.; Cavanagh, A. S.; Riley, L. A.; Kang, S. H.; Dillon, A. C.; Groner, M. D.; George, S. M.; Lee, S. H. Ultrathin Direct Atomic Layer Deposition on Composite Electrodes for Highly Durable and Safe Li-Ion Batteries. *Adv. Mater.* **2010**, *22*, 2172−2176.
(10) Chen, Z.; Qin, Y.; Amine, K.; Sun, Y.-K. Role of Surface Coating on Cathode Materials for Lithium-Ion Batteries. *J. Mater. Chem.* **2010**, *20*, 7606−7612.
(11) Lee, J.-T.; Wang, F.-M.; Cheng, C.-S.; Li, C.-C.; Lin, C.-H. Low-Temperature Atomic Layer Deposited Al_2O_3 Thin Film on Layer Structure Cathode for Enhanced Cycleability in Lithium-Ion Batteries. *Electrochim. Acta* **2010**, *55*, 4002−4006.
(12) Woo, J. H.; Trevey, J. E.; Cavanagh, A. S.; Choi, Y. S.; Kim, S. C.; George, S. M.; Oh, K. H.; Lee, S.-H. Nanoscale Interface Modification of $LiCoO_2$ by Al_2O_3 Atomic Layer Deposition for Solid-State Li Batteries. *J. Electrochem. Soc.* **2012**, *159*, A1120−A1124.
(13) Scott, I. D.; Jung, Y. S.; Cavanagh, A. S.; Yan, Y.; Dillon, A. C.; George, S. M.; Lee, S.-H. Ultrathin Coatings on Nano-$LiCoO_2$ for Li-Ion Vehicular Applications. *Nano Lett.* **2010**, *11*, 414−418.
(14) Riley, L. A.; Van Atta, S.; Cavanagh, A. S.; Yan, Y.; George, S. M.; Liu, P.; Dillon, A. C.; Lee, S.-H. Electrochemical Effects of ALD Surface Modification on Combustion Synthesized $LiNi_{1/3}Mn_{1/3}Co_{1/3}O_2$ as a Layered-Cathode Material. *J. Power Sources* **2011**, *196*, 3317−3324.
(15) Jung, Y. S.; Cavanagh, A. S.; Yan, Y.; George, S. M.; Manthiram, A. Effects of Atomic Layer Deposition of Al_2O_3 on the Li-$[Li_{0.20}Mn_{0.54}Ni_{0.13}Co_{0.13}]O_2$ Cathode for Lithium-Ion Batteries. *J. Electrochem. Soc.* **2011**, *158*, A1298−A1302.
(16) Zhang, X.; Belharouak, I.; Li, L.; Lei, Y.; Elam, J. W.; Nie, A.; Chen, X.; Yassar, R. S.; Axelbaum, R. L. Structural and Electrochemical Study of Al_2O_3 and TiO_2 Coated $Li_{1.2}Ni_{0.13}Mn_{0.54}Co_{0.13}O_2$ Cathode Material Using ALD. *Adv. Energy Mater.* **2013**, *3*, 1299−1307.
(17) Jung, S. K.; Gwon, H.; Hong, J.; Park, K. Y.; Seo, D. H.; Kim, H.; Hyun, J.; Yang, W.; Kang, K. Understanding the degradation

DOI: 10.1021/acsami.5b02572
ACS Appl. Mater. Interfaces 2015, 7, 11599−11603

mechanisms of $LiNi_{0.5}Co_{0.2}Mn_{0.3}O_2$ cathode material in lithium ion batteries. *Adv. Energy Mater.* **2014**, *4*, 1300787.
(18) Lin, F.; Markus, I. M.; Nordlund, D.; Weng, T.-C.; Asta, M. D.; Xin, H. L.; Doeff, M. M. Surface Reconstruction and Chemical Evolution of Stoichiometric Layered Cathode Materials for Lithium-Ion Batteries. *Nat. Commun.* **2014**, *5*.
(19) Perdew, J. P.; Burke, K.; Ernzerhof, M. Generalized Gradient Approximation Made Simple. *Phys. Rev. Lett.* **1996**, *77*, 3865−3868.
(20) Blöchl, P. E. Projector Augmented-Wave Method. *Phys. Rev. B* **1994**, *50*, 17953−17979.
(21) Kresse, G.; Furthmüller, J. Efficient Iterative Schemes for Ab Initio Total-Energy Calculations using a Plane-Wave Basis Set. *Phys. Rev. B* **1996**, *54*, 11169−11186.
(22) Dudarev, S.; Botton, G.; Savrasov, S.; Humphreys, C.; Sutton, A. Electron-Energy-Loss Spectra and the Structural Stability of Nickel Oxide: An LSDA+ U Study. *Phys. Rev. B* **1998**, *57*, 1505−1509.
(23) Zhou, F.; Cococcioni, M.; Marianetti, C. A.; Morgan, D.; Ceder, G. First-Principles Prediction of Redox Potentials in Transition-Metal Compounds with LDA+ U. *Phys. Rev. B* **2004**, *70*, 235121.
(24) Ong, S. P.; Mo, Y.; Richards, W. D.; Miara, L.; Lee, H. S.; Ceder, G. Phase Stability, Electrochemical Stability and Ionic Conductivity of the $Li_{10\pm1}MP_2X_{12}$ (M = Ge, Si, Sn, Al or P, and X = O, S or Se) Family of Superionic Conductors. *Energy Environ. Sci.* **2013**, *6*, 148−156.
(25) Groner, M.; Fabreguette, F.; Elam, J.; George, S. Low-Temperature Al_2O_3 Atomic Layer Deposition. *Chem. Mater.* **2004**, *16*, 639−645.
(26) Aaltonen, T.; Nilsen, O.; Magrasó, A.; Fjellvåg, H. Atomic Layer Deposition of Li_2O−Al_2O_3 Thin Films. *Chem. Mater.* **2011**, *23*, 4669−4675.
(27) Meng, X.; Yang, X. Q.; Sun, X. Emerging Applications of Atomic Layer Deposition for Lithium-Ion Battery Studies. *Adv. Mater.* **2012**, *24*, 3589−3615.
(28) Liu, J.; Sun, X. Elegant Design of Electrode and Electrode/Electrolyte Interface in Lithium-Ion Batteries by Atomic Layer Deposition. *Nanotechnology* **2015**, *26*, 024001.
(29) Myung, S.-T.; Izumi, K.; Komaba, S.; Sun, Y.-K.; Yashiro, H.; Kumagai, N. Role of Alumina Coating on Li−Ni−Co−Mn−O Particles as Positive Electrode Material for Lithium-Ion Batteries. *Chem. Mater.* **2005**, *17*, 3695−3704.
(30) Lee, J.-T.; Wang, F.-M.; Cheng, C.-S.; Li, C.-C.; Lin, C.-H. Low-Temperature Atomic Layer Deposited Al_2O_3 Thin Film on Layer Structure Cathode for Enhanced Cycleability in Lithium-Ion Batteries. *Electrochim. Acta* **2010**, *55*, 4002−4006.
(31) Vargel, C. *Corrosion of Aluminium*; Elsevier: Oxford, U.K., 2004.
(32) Silvi, B.; Savin, A. Classification of Chemical Bonds Based on Topological Analysis of Electron Localization Functions. *Nature* **1994**, *371*, 683−686.
(33) Sanchez, J.; El-Mansy, S.; Sun, B.; Scherban, T.; Fang, N.; Pantuso, D.; Ford, W.; Elizalde, M.; Martınez-Esnaola, J.; Martın-Meizoso, A. Cross-Sectional Nanoindentation: A New Technique for Thin Film Interfacial Adhesion Characterization. *Acta Mater.* **1999**, *47*, 4405−4413.
(34) Jung, S. C.; Han, Y.-K. How Do Li Atoms Pass through the Al_2O_3 Coating Layer during Lithiation in Li-ion Batteries? *J. Phys. Chem. Lett.* **2013**, *4*, 2681−2685.
(35) Liu, Y.; Hudak, N. S.; Huber, D. L.; Limmer, S. J.; Sullivan, J. P.; Huang, J. Y. In Situ Transmission Electron Microscopy Observation of Pulverization of Aluminum Nanowires and Evolution of the Thin Surface Al_2O_3 Layers during Lithiation−Delithiation Cycles. *Nano Lett.* **2011**, *11*, 4188−4194.
(36) Hao, S.; Wolverton, C. Lithium Transport in Amorphous Al_2O_3 and AlF_3 for Discovery of Battery Coatings. *J. Phys. Chem. C* **2013**, *117*, 8009−8013.
(37) Götzmann, O. Thermodynamics of Ceramic Breeder Materials for Fusion Reactors. *J. Nucl. Mater.* **1989**, *167*, 213−224.

DOI: 10.1021/acsami.5b02572
ACS Appl. Mater. Interfaces 2015, 7, 11599−11603